

A Low-Overpotential Potassium–Oxygen Battery Based on Potassium Superoxide

Xiaodi Ren and Yiying Wu*

Department of Chemistry and Biochemistry, The Ohio State University, 100 West 18th Avenue, Columbus, Ohio 43210, United States

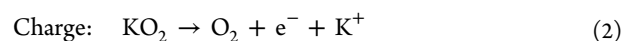
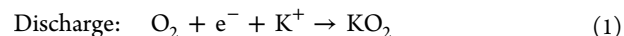
S Supporting Information

ABSTRACT: Li–O₂ battery is regarded as one of the most promising energy storage systems for future applications. However, its energy efficiency is greatly undermined by the large overpotentials of the discharge (formation of Li₂O₂) and charge (oxidation of Li₂O₂) reactions. The parasitic reactions of electrolyte and carbon electrode induced by the high charging potential cause the decay of capacity and limit the battery life. Here, a K–O₂ battery is reported that uses K⁺ ions to capture O₂^{•−} to form the thermodynamically stable KO₂ product. This allows for the battery to operate through the one-electron redox process of O₂/O₂^{•−}. Our studies confirm the formation and removal of KO₂ in the battery cycle test. Furthermore, without the use of catalysts, the battery shows a low discharge/charge potential gap of less than 50 mV at a modest current density, which is the lowest one that has ever been reported in metal–oxygen batteries.

Recently, lithium–oxygen batteries have received considerable attention from researchers due to their high specific energy.^{1–5} Nonaqueous lithium–oxygen battery, which is based on the net reaction of 2Li + O₂ ↔ Li₂O₂ (E⁰ = 2.96 V), has a theoretical specific energy as high as 3505 W·h/kg.^{2,6} However, lithium–oxygen battery research is facing a lot of challenges. The discharge process involves the reduction of oxygen to superoxide (O₂^{•−}), the formation of LiO₂ and its disproportionation into Li₂O₂ and O₂; while the charge process is the direct oxidation of Li₂O₂ into O₂.⁷ As a result of the asymmetric reaction mechanism, battery charge has a much higher overpotential (~1–1.5 V) than that of discharge (~0.3 V), which renders the system with a low round-trip energy efficiency around 60%. Recently, researchers have also found out the instability of electrolyte and carbon electrode under the high charging potential (>3.5 V), which contributes to the low rechargeability.^{8–10} Different electrocatalysts have been explored to lower the overpotentials.^{11,12} But the necessity of catalysts has been argued, because the catalyst on carbon may not be able to work once its surface is blocked.¹³ Moreover, side reactions can be facilitated by the catalysts.¹⁴ On the other hand, the insulating nature of bulk Li₂O₂ (band gap larger than 4 eV, calculated values^{15,16}) can hinder the charge transfer reactions and result in a limited battery capacity. It has been shown experimentally that charge transport through the Li₂O₂ film would be largely suppressed once the film thickness exceeds 5–10 nm.¹⁷

Therefore, new chemistry is needed to solve the problems in Li–O₂ batteries. The O₂/O₂^{•−} redox couple has been shown to be quasi-reversible in aprotic solvents.^{18,19} It agrees with our prediction of a lower energy barrier for the conversion from O₂^{•−} to O₂ than that from O₂^{2−} to O₂, given the fact that O₂^{•−} has a closer bond length (1.28–1.33 Å) to O₂ (1.21 Å) than that of O₂^{2−} (~1.49 Å).^{20,21} However, a key problem in Li–O₂ batteries is that LiO₂ is unstable due to the high charge density of Li⁺. On the basis of the Hard–Soft Acid–Base (HSAB) theory, O₂^{•−} is more stable with cation of a lower charge density.¹⁸ In contrast with LiO₂ and NaO₂, KO₂ is thermodynamically stable and commercially available.

Electrochemical measurements were carried out first to verify the influence of cations on the redox chemistry of oxygen. Figure 1a shows our cyclic voltammetry studies of the oxygen reduction reaction in an aprotic solvent with the presence of different cations. The oxygen reduction and oxidation potential gap in the electrolyte with K⁺ is much smaller than that in the electrolyte with Li⁺. This implies that a K–O₂ battery may operate at much lower overpotentials and thus has a higher round-trip energy efficiency than a Li–O₂ battery. The larger cathodic peak than the anodic peak with K⁺ may result from the passivation of the electrode by K₂O₂, which is formed by the further reduction of KO₂, as the potential for K₂O₂ formation is only 0.28 V lower than that of KO₂ (see Table S1 and Figure S1 for details). Therefore, a large negative polarization of the electrode should be avoided to prevent the formation of K₂O₂. Within a controlled potential range, the reactions on the porous carbon electrode is then expected to occur as follows:



The net battery reaction is K + O₂ ↔ KO₂ (ΔG⁰ = −239.4 kJ/mol, E⁰ = 2.48 V),²² which gives a theoretical energy density of 935 W·h/kg (based on the mass of KO₂).

To verify the hypothesis, a Swagelok K–O₂ battery was fabricated, containing a potassium metal foil, a glassy fiber separator and a porous carbon electrode (Super P carbon powders with binder in a Ni foam framework, see Supporting Information, SI). We used 0.5 M KPF₆ in an ether solvent (1,2-dimethoxyethane (DME) or diglyme) as the electrolyte. For comparison, a Li–O₂ battery was built in a similar manner (electrolyte: 1 M LiCF₃SO₃ in tetraglyme). The electro-

Received: December 10, 2012

Published: February 12, 2013

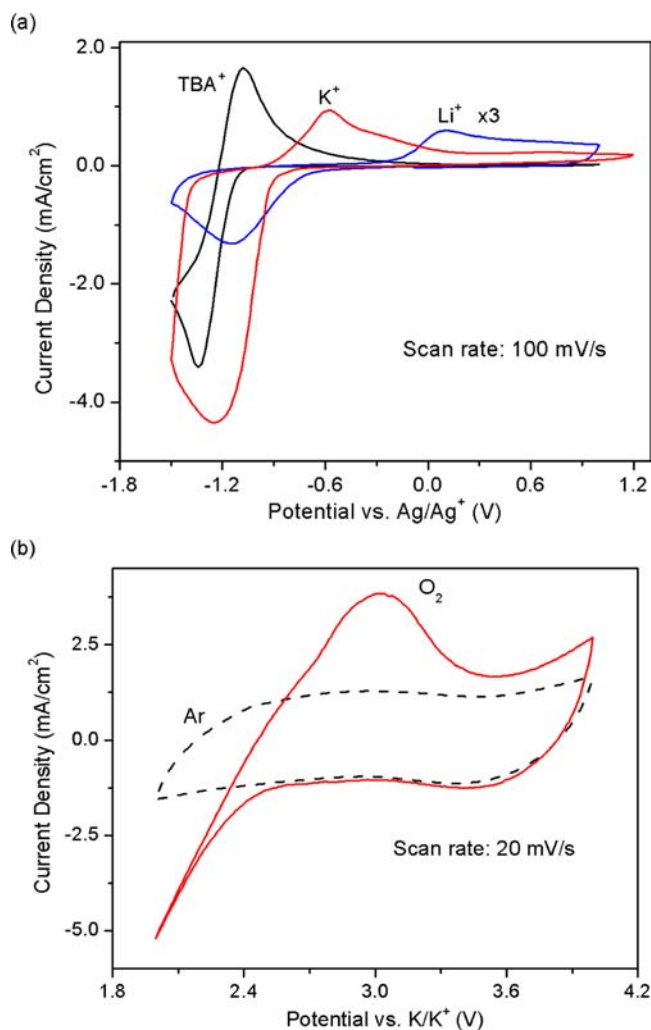


Figure 1. Cyclic voltammograms for oxygen reduction and oxidation. (a) On a glassy carbon electrode in oxygen saturated acetonitrile containing 0.1 M TBAPF₆, LiClO₄ or KPF₆ (three-electrode setup). Current density for the LiClO₄ electrolyte was enlarged three times for clarity. A good reversibility of the O₂/O₂⁻ couple can be observed with tetrabutylammonium cation (TBA⁺) due to its large size and thus low charge density. (b) On a porous carbon electrode in DME with 0.5 M KPF₆ (two-electrode battery setup). Oxygen pressure is one atm.

chemical behavior (Figure 1b) of the carbon cathode in the K–O₂ battery was investigated by cyclic voltammetry in the two-electrode battery setup (K metal as the counter and reference electrode). Before oxygen was purged into the battery, only the double layer capacitor behavior of carbon was observed. Oxygen reduction and oxidation processes could be clearly seen when oxygen was introduced into the battery. The difference between the onset potentials of oxygen reduction and oxidation is very small. The oxidation process at the potential higher than 3.5 V is attributed to the decomposition of carbon electrode or electrolyte, which agrees with the recent study.¹⁰ This indicates that the oxidation process can be complete within the potential range where the carbon electrode and the electrolyte are relatively stable.

The first discharge and charge voltage profiles of our K–O₂ battery and Li–O₂ battery are shown in Figure 2a. The stable discharge plateau is at 2.70 V (overpotential $\eta_{\text{dischrg}} = 260$ mV) for the Li–O₂ battery and at 2.47 V ($\eta_{\text{dischrg}} \sim 10$ mV) for the K–O₂ battery. The smaller discharge overpotential of the K–

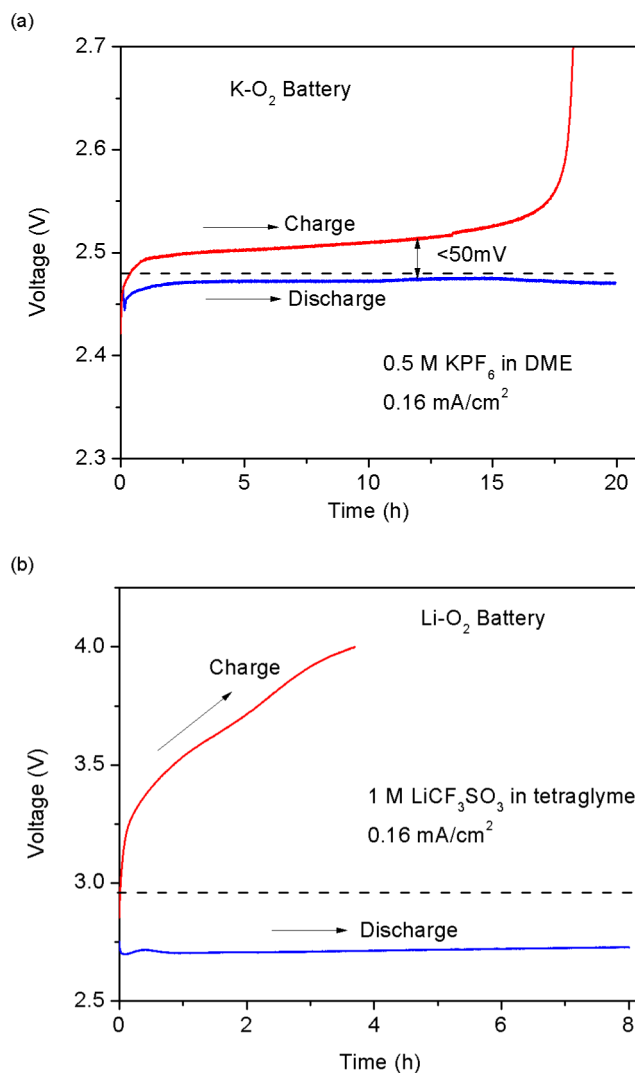


Figure 2. Voltage curves of the first discharge–charge cycle. (a) K–O₂ battery (0.5 M KPF₆ in DME). The K metal electrode was replaced by a fresh one after the first discharge process. (b) Li–O₂ battery (1 M LiCF₃SO₃ in tetraglyme). Both at a current density of 0.16 mA/cm². Electrode geometric area is 0.64 cm². The dash lines indicate the calculated thermodynamic potentials for the batteries.

O₂ battery may result from the better conductivity of KO₂ (>10 S/cm², room temperature²³) than Li₂O₂. More importantly, in the subsequent charging process, the voltage is as low as 2.50–2.52 V for the K–O₂ battery. The charge overpotential η_{chrg} of ~ 20 –40 mV is significantly smaller than the Li–O₂ battery. Moreover, within this small charging potential range, almost 90% of the discharged product can be oxidized. In contrast, for the Li–O₂ battery, only half of the product was able to be removed even when the voltage reaches 4.0 V, where the ether electrolyte and the carbon electrode become unstable. The charge/discharge potential gap of about 50 mV is the lowest one that has ever been reported in metal–oxygen batteries. Compared with the typical Li–O₂ battery, which has a potential gap larger than 1 V, our K–O₂ battery can provide an exceptional round-trip energy efficiency of >95%.

To prove the formation and removal of KO₂ in battery cycle, the discharged and the recharged cathodes were characterized by X-ray diffraction and Raman spectroscopy. As shown in Figure 3a, crystalline KO₂ was confirmed as the dominant

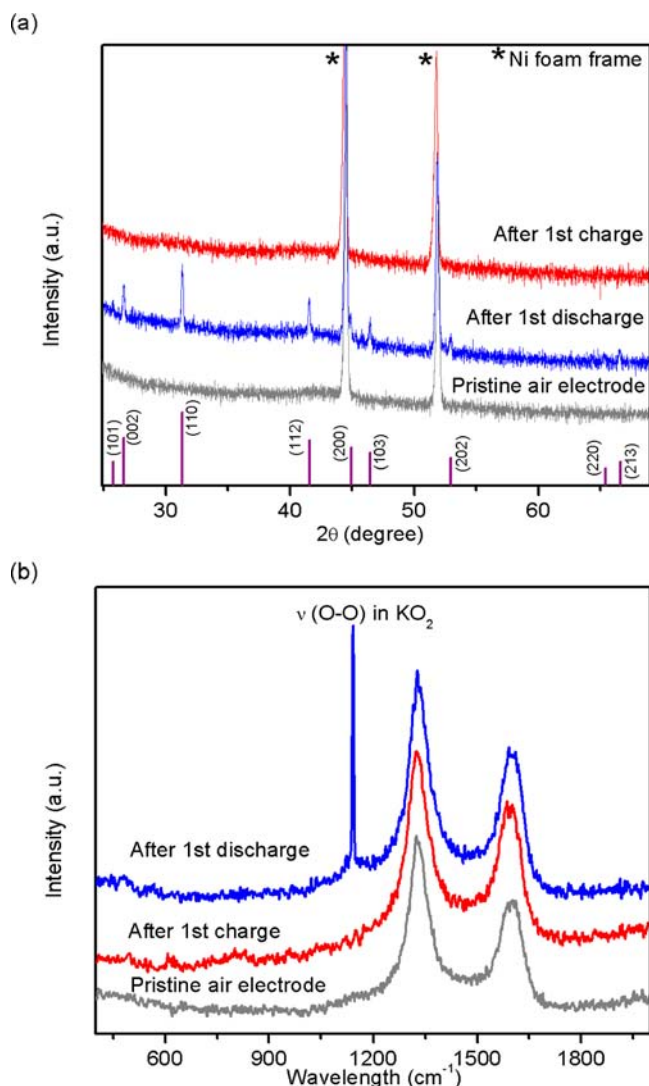


Figure 3. Characterization of carbon electrodes of the K–O₂ battery. (a) XRD patterns of a pristine air electrode, one after first discharge process and one after first charge process. The lines represent the standard XRD pattern of KO₂ (JCPDS No. 43-1020). (b) Raman spectra of a pristine air electrode, one after first discharge process and one after first charge process.

discharge product, and the peaks match well with the standard pattern (JCPDS No. 43-1020). No evidence of other potassium oxides, such as potassium peroxide (K₂O₂) or potassium oxide (K₂O), can be seen. The Raman spectrum of the cathode in Figure 3b also shows the characteristic intense peak of KO₂ at 1142 cm⁻¹.^{24,25} The other two broad peaks come from the G band (1582 cm⁻¹) and D band (1350 cm⁻¹) of the carbon material in the electrodes. Meanwhile, after the battery was recharged, the XRD peaks and Raman signal of KO₂ disappeared, which confirms that KO₂ was oxidized during charging.

The oxidation of KO₂ at a low overpotential was also proved by charging an artificially discharged electrode. The electrode was prepared by loading slurry of hand-milled KO₂, carbon powder and binder (weight ratio = 1:2:1) into Ni foam. The main process stays within a low voltage range between 2.55 and 2.90 V, as in Figure 4. Without KO₂, the voltage goes beyond 4.0 V in less than 10 min (data not shown here), which shows the reaction here is the oxidation of KO₂, not the oxidation of

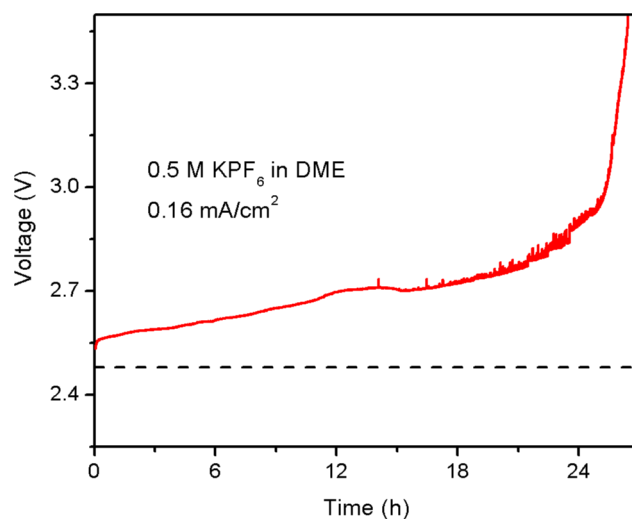


Figure 4. The charging process of a KO₂-loaded battery at 0.16 mA/cm² current density.

the electrolyte. The higher potential than that shown in Figure 2a is believed to come from the fact that the electronic contact between this mechanically mixed KO₂ and carbon is not as good as that formed in electrochemical reactions. The amount of KO₂ calculated from the total charge flow in the oxidation process is ~6.9 mg, and the amount of loaded KO₂ is 8.0 mg. Their small difference may be due to the fact that some of the initial KO₂ particles loosely bound to carbon particles stay unreacted. The XRD characterization of the electrode after the charging process (Figure S2) shows only the peaks of the substrate Ni foam with no apparent KO₂ peaks left, which verifies that the reaction in the charging process is the oxidation of KO₂.

Our K–O₂ battery shows several cycles of rechargeability, although the capacity decays with increasing cycle number. As shown in Figure 5, the discharge capacity of the second cycle is only half of the first cycle, and the charge voltage is also higher. Without the degradation of the electrolyte, the reactivity of potassium with electrolyte is not a major issue for battery rechargeability. As shown in Figure S3, the voltage profile of the

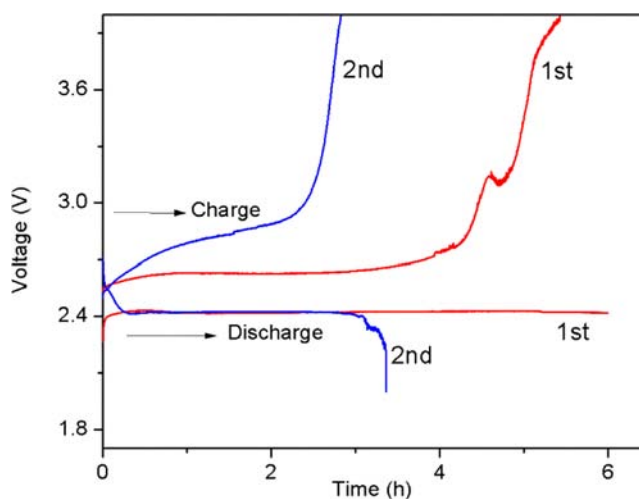


Figure 5. The first two continuous battery discharge–charge cycles at 0.16 mA/cm² current density. (0.5 M KPF₆ in butyl diglyme/diglyme mixture with volume ratio 2:5.)

potassium electrodeposition and electrodisolution cycles shows only a slight change (about 9 mV) during 10 cycles in 20 h. However, the recyclability of our K–O₂ battery greatly suffers from the same electrolyte stability issue as the Li–O₂ battery, which is induced by the reactive superoxide ions reacting with the ether solvent. Species such as H₂O, potassium formate (HCOOK) and potassium acetate (CH₃COOK) (both were identified from the NMR test after battery discharge, see Figure S4. HCO₂D, δ = 8.47 ppm, singlet; CH₃CO₂D, δ = 1.93 ppm, singlet) should be the main side products, following the mechanism discussed in a previous study.²⁶

When the side products diffuse to the metal electrode, they can easily react with potassium and form an insulating layer on the metal surface, which was observed when the batteries were taken apart after tests. As a result, it is still challenging to get a good cycle life for the K–O₂ battery. When the same K electrode was used, the insulating layer on K metal surface would accumulate. Therefore, the voltage of the second charging process is higher than the voltage of the first charging process. Moreover, even a short charging process would result in apparent growth of the surface layer thickness, and then limited the capacity in the second discharge process. Our detailed studies of the degradation mechanism, particularly the solvent effect, are underway.

In conclusion, a major obstacle for developing highly efficient Li–O₂ batteries lies in the large overpotentials of the electrochemical reactions. Here, we have demonstrated the concept of a K–O₂ battery with low overpotentials by taking advantage of the reversibility of the O₂/O₂^{•−} redox couple. A charge/discharge potential gap smaller than 50 mV at a current density of 0.16 mA/cm² is reported for the first time. XRD and Raman have confirmed the formation and removal of KO₂ in the battery cycle test.

As a final note, very recently during the preparation of this paper, another group of researchers has published their results about a Na–O₂ battery.²⁷ Although it shares a similar mechanism with our K–O₂ battery, a notable difference is that KO₂ is both kinetically and thermodynamically stable, while NaO₂ is only kinetically stable. This can bring some advantages to our K–O₂ battery. For example, as shown earlier, a KO₂-loaded carbon electrode can be prepared as the artificially discharged cell, which allows us to separately study the charging step and the discharging step. This is helpful for an in-depth understanding of the battery processes. Despite this difference, the promising results from both K–O₂ and NaO₂ batteries indicate the potential of the superoxide batteries.

■ ASSOCIATED CONTENT

📄 Supporting Information

Experimental procedures and supporting figures. This material is available free of charge via the Internet at <http://pubs.acs.org>.

■ AUTHOR INFORMATION

Corresponding Author

wu@chemistry.ohio-state.edu

Notes

The authors declare no competing financial interest.

■ ACKNOWLEDGMENTS

This work was supported by NSF (CAREER, DMR-0955471) and also in part by The Ohio State University Materials Research Seed Grant Program.

■ REFERENCES

- (1) Abraham, K. M.; Jiang, Z. *J. Electrochem. Soc.* **1996**, *143*, 1.
- (2) Bruce, P.; Freunberger, S. *Nat. Mater.* **2011**, *11*, 31.
- (3) Ogasawara, T.; Débart, A.; Holzapfel, M.; Novák, P.; Bruce, P. G. *J. Am. Chem. Soc.* **2006**, *128*, 1390.
- (4) Jung, H.; Hassoun, J.; Park, J.; Sun, Y.; Scrosati, B. *Nat. Chem.* **2012**, *4*, 579.
- (5) Girishkumar, G.; McCloskey, B.; Luntz, A. C.; Swanson, S.; Wilcke, W. *J. Phys. Chem. Lett.* **2010**, *1*, 2193.
- (6) Lu, Y.-C.; Gasteiger, H. A.; Parent, M. C.; Chiloyan, V.; Shao-Horn, Y. *Electrochem. Solid-State Lett.* **2010**, *13*, A69.
- (7) Peng, Z.; Freunberger, S. A.; Hardwick, L. J.; Chen, Y.; Giordani, V.; Bardé, F.; Novák, P.; Graham, D.; Tarascon, J.-M.; Bruce, P. G. *Angew. Chem., Int. Ed.* **2011**, *50*, 6351.
- (8) Xu, W.; Hu, J.; Engelhard, M. H.; Towne, S. A.; Hardy, J. S.; Xiao, J.; Feng, J.; Hu, M. Y.; Zhang, J.; Ding, F.; Gross, M. E.; Zhang, J.-G. *J. Power Sources* **2012**, *215*, 240.
- (9) McCloskey, B.; Scheffler, R. *J. Phys. Chem. C* **2012**, *116*, 23897.
- (10) Ottakam Thotiyl, M. M.; Freunberger, S. A.; Peng, Z.; Bruce, P. G. *J. Am. Chem. Soc.* **2013**, *135*, 494.
- (11) Débart, A.; Paterson, A. J.; Bao, J.; Bruce, P. G. *Angew. Chem., Int. Ed.* **2008**, *47*, 4521.
- (12) Cao, R.; Lee, J.-S.; Liu, M.; Cho, J. *Adv. Energy Mater.* **2012**, *2*, 816.
- (13) McCloskey, B. D.; Scheffler, R.; Speidel, A.; Bethune, D. S.; Shelby, R. M.; Luntz, A. C. *J. Am. Chem. Soc.* **2011**, *133*, 18038.
- (14) Black, R.; Oh, S. H.; Lee, J.; Yim, T.; Adams, B.; Nazar, L. F. *J. Am. Chem. Soc.* **2012**, *134*, 2902.
- (15) Hummelshøj, J. S.; Blomqvist, J.; Datta, S.; Vegge, T.; Rossmeisl, J.; Thygesen, K. S.; Luntz, A. C.; Jacobsen, K. W.; Nørskov, J. K. *J. Chem. Phys.* **2010**, *132*, 071101.
- (16) Ong, S. P.; Mo, Y.; Ceder, G. *Phys. Rev. B* **2012**, *85*, 081105.
- (17) Viswanathan, V.; Thygesen, K. S.; Hummelshøj, J. S.; Nørskov, J. K.; Girishkumar, G.; McCloskey, B. D.; Luntz, A. C. *J. Chem. Phys.* **2011**, *135*, 214704.
- (18) Laoire, C. O.; Mukerjee, S.; Abraham, K. M.; Plichta, E. J.; Hendrickson, M. A. *J. Phys. Chem. C* **2010**, *114*, 9178.
- (19) Laoire, C. O.; Mukerjee, S.; Abraham, K. M.; Plichta, E. J.; Hendrickson, M. A. *J. Phys. Chem. C* **2009**, *113*, 20127.
- (20) Dietzel, P. D. C.; Kremer, R. K.; Jansen, M. *J. Am. Chem. Soc.* **2004**, *126*, 4689.
- (21) Föppel, H. *Z. Anorg. Allg. Chem.* **1957**, *291*, 12–50.
- (22) *CRC Handbook of Chemistry and Physics*; Haynes, W. M., Ed.; 93rd ed.; CRC Press/Taylor and Francis: Boca Raton, FL, 2013.
- (23) Khan, A. U.; Mahanti, S. D. *J. Chem. Phys.* **1975**, *63*, 2271.
- (24) Smardzewski, R. R. *J. Chem. Phys.* **1972**, *57*, 1327.
- (25) Andrews, L. *J. Chem. Phys.* **1971**, *54*, 4935.
- (26) Freunberger, S. A.; Chen, Y.; Drewett, N. E.; Hardwick, L. J.; Bardé, F.; Bruce, P. G. *Angew. Chem., Int. Ed.* **2011**, *50*, 8609.
- (27) Hartmann, P.; Bender, C. L.; Vračar, M.; Dürr, A. K.; Garsuch, A.; Janek, J.; Adelhelm, P. *Nat. Mater.* **2012**, DOI: 10.1038/nmat3486.